JOURNAL OF AGRICULTURAL AND FOOD CHEMISTRY
ARTICLE

J. Agric. Food Chem. 2010, 58, 2377–2387 2377
DOI:10.1021/jf903514t

Structural Makeup, Biopolymer Conformation, and Biodegradation Characteristics of a Newly Developed Super Genotype of Oats (CDC SO-I versus Conventional Varieties): A Novel Approach

Daalkhaijav Damiran and Peiqiang Yu*

Department of Animal and Poultry Science, College of Agriculture and Bioresources, University of Saskatchewan, 51 Campus Drive, Saskatoon, Saskatchewan, Canada S7N 5A8

Recently, a new "super" genotype of oats (CDC SO-I or SO-I) has been developed. The objectives of this study were to determine structural makeup (features) of oat grain in endosperm and pericarp regions and to reveal and identify differences in protein amide I and II and carbohydrate structural makeup (conformation) between SO-I and two conventional oats (CDC Dancer and Derby) grown in western Canada in 2006, using advanced synchrotron radiation based Fourier transform infrared microspectroscopy (SRFTIRM). The SRFTIRM experiments were conducted at National Synchrotron Light Sources, Brookhaven National Laboratory (NSLS, BNL, U.S. Department of Energy). From the results, it was observed that comparison between the new genotype oats and conventional oats showed (1) differences in basic chemical and protein subfraction profiles and energy values with the new SO-I oats containing lower lignin (21 g/kg of DM) and higher soluble crude protein (530 g/kg CP), crude fat (59 g/kg of DM), and energy values (TDN, 820 g/kg of DM; NE_{L3x}, 7.8 MJ/kg of DM); (2) significant differences in rumen biodegradation kinetics of dry matter, starch, and protein with the new SO-I oats containing lower EDDM (638 g/kg of DM) and higher EDCP (103 g/kg of DM); (3) significant differences in nutrient supply with highest truly absorbed rumen undegraded protein (ARUP, 23 g/kg of DM) and total metabolizable protein supply (MP, 81 g/kg of DM) from the new SO-I oats; and (4) significant differences in structural makeup in terms of protein amide I in the endosperm region (with amide I peak height from 0.13 to 0.22 IR absorbance unit) and cellulosic compounds to carbohydrate ratio in the pericarp region (ratio from 0.02 to 0.06). The results suggest that with the SRFTIRM technique, the structural makeup differences between the new genotype oats (SO-I) and two conventional oats (Dancer and Derby) could be revealed.

KEYWORDS: Structural makeup; biopolymer conformation; biodegradation kinetics; modeling nutrient supply; oats

INTRODUCTION

In Canada, oat (*Avena sativa* L.) is the third most important cereal crop after wheat and barley; the total stock estimate for oats was 2.0 million tons in 2008, an increase of 30.3% from 2007 and substantially above the five-year average of 1.6 million tons (*1*). Oat use in the human food sector has recently increased because of the positive health benefit attributed to oat (*2*), but ruminant livestock feeding remains the primary use of oat grain. In parallel, with the recent increase in feed grain prices (due to an dramatic increase of bioethanol production), less wheat and barley grains are available as livestock feed. Oat should receive serious consideration for more inclusion in animal feed. The feed value of oat grain has been considered inferior to that of barley (*3*). This is mainly due to the hull content of oat, which ranges from 20 to 30% (*4*). Oat hulls are fibrous and contain substantial amounts of indigestible lignin (*5*). For this reason, nutritional improvements to oat will need to be made before oat grain becomes a favored feed for ruminants.

Recently, a new "super" genotype of oat variety CDC SO-I (SO-I) has been developed by the Crop Development Centre's oat breeding program, University of Saskatchewan, Canada, using a pedigree breeding system. It originated from the cross AC Assiniboia × SA96121. Selection criteria for SO-I included high yield potential, early maturity, straw strength, disease resistance (B. Rossnagel, personal communication), and grain quality including the combination of low acid detergent lignin hull and high oil groat characteristics. Recently published results showed that the SO-I would be a good cereal grain for feeding lactating dairy cows and can be fed whole, without any loss of performance in calf backgrounding diets in western Canada (*6*, *7*).

Why does the new SO-I oat differ from conventional oats in terms of animal performance? Is it because the molecular structural makeup was different between the oats? This was a question that needed to be answered. Currently, data on molecular structural

*Corresponding author [telephone (306) 966-4132; e-mail peiqiang.yu@usask.ca].

Published on Web 01/22/2010

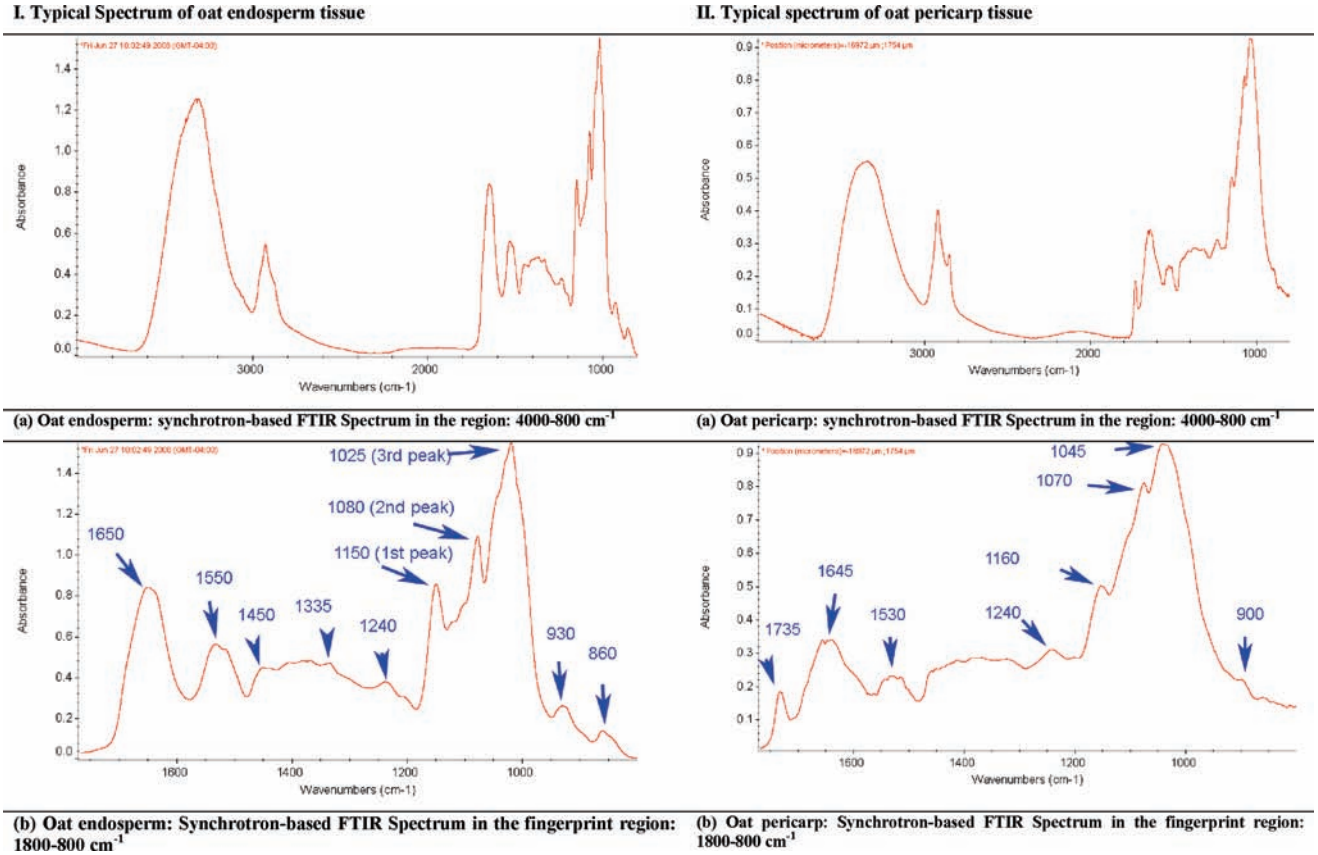

Figure 1. Synchrotron-based FTIR spectrum in oat seed endosperm and pericarp tissues (pixel size: 10 μm × 10 μm): (**a**) whole region, ca. 4000−800 cm^{-1}; (**b**) fingerprint region, ca. 1800−800 cm^{-1}; (**c**) protein amide I region, 1720−1575 cm^{-1}; (**d**) protein amide II region, 1575−1485 cm^{-1}; (**e**) total carbohydrate region, ca. 1185−800 cm^{-1}; (**f**) nonstructural carbohydrate (starch) region, ca. 1065−950 cm^{-1}.

makeup (features/conformation) at a cellular level of this new variety of oats are limited, in comparison with the conventional oat varieties. Advanced synchrotron radiation based FTIR microsepctroscopy (SRFTIRM), taking advantage of bright synchrotron light (a million times brighter than sunlight), is capable of detecting structure information at both cellular and molecular levels within intact biological tissues. SRFTIRM can provide four kinds of information simultaneously: tissue chemistry, tissue composition, tissue environment, and tissue structure. Detailed advantages, applications of SRFTIRM, why wet chemical analysis fails to detect feed structural feature, and the need for SRFTIRM for feed inherent structure research have been reported in *British Journal of Nutrition* (*8*).

The objectives of this study were to use advanced SRFTIRM to determine structural makeup (features/conformation) of the new oats in the endosperm and pericarp tissues and to reveal and identify differences in protein amides I and II and carbohydrate structural makeup between the new genotype oats (SO-I) and two conventional oats (CDC Dancer and Derby). The items assessed included (1) structural differences in protein amide I and II intensity and their ratios within cellular dimensions; (2) structural differences in carbohydrate and component peak intensity ratio within cellular dimensions; (3) structural differences in amides to carbohydrate intensity ratio within cellular dimensions; and (4) chemical and biological differences (biodegradation kinetics) and nutrient supply (a modeling approach) between the new super genotype oats (SO-I) and two conventional oats (Dancer and Derby).

MATERIALS AND METHODS

Sample Preparation: Newly Developed Genotype of Oats and Conventional Oat Varieties. The newly developed genotype of oats (SO-I) and two conventional oat varieties (Dancer and Derby), grown at the University of Saskatchewan research station (Saskatoon) in 2006, were supplied by B. R. Rossnagel, Crop Development Centre (CDC), University of Saskatchewan (Saskatoon, Canada). Dancer is a low hulled, early maturing, milling oat. Derby is a low hulled, midseason type, white-chaffed, milling/forage type oat, and SO-I is a hulled, yellow to light brown kerneled, spring, and forage type oat. The samples were ground through a 0.5 mm screen for starch analysis and through a 1 mm screen for other chemical analyses [Retsch ZM-1, Brinkmann Instruments (Canada) Ltd., Ontario, Canada]. For rumen kinetics in situ study, the oats were processed through a 0.533 mm gap roller mill (model GR, Robin-Dodwell Manufacturing Ltd., Calgary, AB, Canada) at the Engineering Laboratory, University of Saskatchewan (Saskatoon, SK, Canada).

Biological Differences Determination Using an in Situ Rumen Incubation Technique. Ruminal degradation characteristics were determined using the in situ method (*9*). Two Holstein dairy cows fitted with rumen cannula were used for measuring rumen degradation characteristics. The animals in this study were cared for in accordance with guidelines established by the Canadian Council on Animal Care in 1990. Seven grams of an individual ground sample was weighed into each preweighed and numbered nylon bag (10 × 20 cm) with the pore size of approximately 40 μm. These bags were tied about 2 cm below the top, allowing a ratio of sample size to bag surface area of 28 mg/cm^2. The rumen incubations were performed according to the "gradual addition/all out" schedule. Samples were incubated in the rumen for 0, 2, 4, 8, 12, 24, and 48 h. The multibags for each treatment and each incubation times were 2, 2, 2, 2, 3, 4, and 5 bags for incubation times 0, 2, 4, 8, 12, 24, and 48 h, respectively. After incubation, the bags were removed from rumen and rinsed under a cold stream of tap water to remove excess ruminal contents. The bags were washed with cool water without detergent and subsequently dried at 55 °C for 48 h. The 0 h incubation samples were only washed under the same conditions. Dry samples were stored in a refrigerated room (4 °C) until analysis. The residues were pooled according to oat variety, incubation time, and animal for laboratory chemical analysis.

Table 1. Basic Chemical Composition, Protein Subfractions, and Energy Values of the Oats: Comparison of Newly Developed SO-I Oat with Normal Oats (Dancer and Derby) Grown at the University of Saskatchewan Research Station (Saskatoon) in 2006

	oats		
item	Dancer	Derby	SO-I (super oat)
chemical and nutrient profiles			
DM (g/kg)	939	937	942
ash (g/kg of DM)	32	32	37
CFat (g/kg of DM)	46	43	59
NDF (g/kg of DM)	279	277	322
ADF (g/kg of DM)	119	133	143
ADL (g/kg of DM)	40	33	21
starch (g/kg of DM)	468	389	452
protein characteristics			
CP (g/kg of DM)	120	116	127
SCP(g/kg of CP)	402	475	530
NPN (g/kg of SCP)	304	170	216
NPN (g/kg of CP)	122	81	114
ADICP (g/kg of CP)	70	38	32
NDICP (g/kg of CP)	131	60	67
protein subfractions			
PA (g/kg of CP)	122	81	114
PB1 (g/kg of CP)	279	394	415
PB2 (g/kg of CP)	467	466	403
PB3 (g/kg of CP)	61	22	35
PC (g/kg of CP)	70	38	32
energy value (MJ/kg of DM; NRC-2001 Dairy and NRC-1996 Beef)			
$TDN_{1\times}$ (g/kg of DM)	797	801	820
$NE_{L3\times}$ (NRC-2001 dairy)	7.5	7.5	7.8
NE_m (NRC-1996 beef)	8.1	8.1	8.4
NE_g (NRC-1996 beef)	5.4	5.4	5.6

Chemical Analysis. The dry matter (DM), ash, crude fat (CFat), and crude protein (CP) contents were analyzed according to the procedure of AOAC (*10*). The acid detergent fiber (ADF), neutral detergent fiber (NDF), and acid detergent lignin (ADL) values were analyzed according to the procedures of Van Soest et al. (*11*). For determination of NDF, ADF, and ADL, an ANKOM Fiber Analyzer was used. The starch was analyzed using the Megazyme Total Starch Assay Kit (Megazyme International Ireland Ltd., Wicklow, Ireland). The nonprotein nitrogen (NPN) content was obtained by precipitation of true protein in the filtrate with trichloroacetic acid (final concentration = 10%) and determined as the difference between total N and the N content of the residue after filtration. The amount of CP associated with NDF (NDICP) and ADF (ADICP) was determined by analyzing the NDF and ADF residues for CP (*10*).

Rumen Biodegradation Kinetics. Rumen degradation characteristics of DM, CP, and starch were determined by the in situ method. In this technique, the results were calculated using the NLIN procedure of the SAS using iterative least-squares regression (Gauss−Newton method) by the following the first-order kinetics equations: $R(t) = U + D \times \exp(-K_d \times (t - T_0))$ for DM and CP and $R(t) = D \times \exp(-K_d \times t)$ for starch (*12*), where $R(t)$ stands for residue of the incubated material after t h of rumen incubation (g/kg); U and D stand for the undegradable and potentially degradable fractions, respectively (in g/kg); T_0 is lag time (h); and K_d is the degradation rate (h^{-1}). The effective degradability (ED) values were calculated as: EDCP (EDDM or EDST) (g/kg) = $S + D \times K_d/(K_p + K_d)$; EDCP (g/kg of DM) = CP (g/kg of DM) × EDCP (g/kg); EDST (g/kg of DM) = ST (g/kg of DM) × EDST (g/kg), where soluble fraction (S) in g/kg and passage rate (K_p) of 0.06 h^{-1} were adopted (*12*). The rumen undegradable feed protein (RUP) value was calculated as RUP (g/kg) = $U + D \times K_p/(K_p + K_d)$ and RUP (g/kg of DM) = 1.11 × CP (g/kg of DM) × RUP (g/kg), where K_p of 0.06 h^{-1} was adopted. The rumen undegraded feed starch (RUST) values were calculated as RUST (g/kg) = $D \times K_p/(K_p + K_d) + 0.1 \times S$ and RUST (g/kg of DM) = ST (g/kg of DM) × RUST (g/kg), where K_p of 0.06 h^{-1} was adopted (*12*). For the factor 0.1 in the formula, it was assumed that for starch, 100 g/kg of soluble fraction (S) escapes rumen fermentation (*12*).

Modeling Nutrient Supply from the Oats. The potential nutrient supply from the oats in terms of (1) truly absorbed rumen undegraded feed protein in the small intestine (ARUP, g/kg of DM), (2) truly absorbed rumen synthesized microbial protein in the small intestine (AMC, g/kg of DM), (3) total truly absorbed protein in the small intestine, (4) total metabolizable protein (MP), and (5) degradable protein balance (OEB in DVE/OEB model, PBD in NRC model) was modeled according to the DVE/OEB system and the NRC-2001 model.

Using Synchrotron Radiation Based FTIR Microspectroscopy (SRFTIRM) on Inherent Structural Chemical Makeup Analysis. Structural−chemical makeup analysis in different types of cereal grains was carried out using the SRFTIRM method described by Yu (*8*) and Yu et al. (*13*). This technique takes advantage of synchrotron light brightness and is capable of exploring the molecular chemistry within microstructures of biological samples with high signal-to-noise ratio at ultraspatial resolutions as fine as 3−10 μm. SRFTIRM is able to identify molecular constituents in biological samples from their vibration spectra in the mid-IR region. A simplified explanation of this technique is when IR passes through a sample, different functional groups and bonds of molecules of biological components absorb (vibrate spectra) IR light independently and some IR passes through. By measuring these different IR absorption characteristics (fingerprint: i.e., absorbed intensity, intensity ratios, and spectral pattern), it is possible to determine if functional groups (such as amide I, aromatic compound, carbonyl ester) exist in particular biological tissues.

Synchrotron Sample Preparation, Light Sources, and SRFTIRM. Three varieties of oat, Dancer, Derby, and SO-I, were tested. The seeds were cut into thin cross sections (ca. 6 μm thick) using a microtome at Western College of Veterinary, University of Saskatchewan, Saskatoon, Canada. The synchrotron experiments were performed at the National Synchrotron Light Source in Brookhaven National Laboratory (NSLS-BNL; U.S. Department of Energy, New York). The unstained cross sections of the oat grain tissues were mounted onto BaF_2 windows for transmission mode SRFTIRM work. The spectroscopic data were collected using a Nicolet Magna 860 synchrotron radiation-sourced Fourier transform infrared (IR) microspectroscopy (Thermo Nicolet Instruments, Madison, WI) equipped with a Continuum IR microscope with a Schwartzshild 32× objective and a 10× condenser. The bench was configured with a collimated synchrotron light beamline at the NSLS-BNL, which served as an external input to the Nicolet Magna 860. Spectra were collected in the mid-IR range of 4000−800 cm^{-1} at a resolution of 4 cm^{-1} with 128 co-added scans and the aperture setting of 10 × 10 μm. Stage control, spectrum data collection, and processing were performed using OMNIC software 7.3.

Synchrotron-Based FTIR Spectral Data Collection and Analysis. From oat grain windows, the spectra were collected from two important regions: (a) pericarp region and (b) endosperm region. Spectral data were analyzed using both univariate and multivariate molecular spectral analyses (*14*, *15*) to classify the seed inherent structures between the newly developed SO-I and two conventional oat varieties.

Univariate Molecular Spectral Analysis. The spectral data were analyzed using OMNIC software 7.3. Each biological component has an unique molecular chemical−structural feature; each has its own unique IR spectrum. Spectral features associated with protein and total, structural, and nonstructural carbohydrates were assigned according to previous publications (*16*−*24*).

In the endosperm region, protein amide I (1650 cm^{-1}, C═O and C—N stretching vibration), amide II (1650 cm^{-1}; N—H bending and C—N stretching vibration), total amides I and II, total carbohydrate (1180−800 cm^{-1}, CHO; C—O stretching vibration), and carbohydrate component peaks and their ratio were analyzed according to the peak area and height intensities (**Figure 1**). For protein amide I analysis, the peak baseline was ca. 1728−1483 cm^{-1} and the region was 1745−1579 cm^{-1}. For protein amide II analysis, the peak baseline was ca. 1728−1483 cm^{-1} and the region was 1579−1485 cm^{-1}. For the CHO analysis, the peak baseline was ca. 1180−800 cm^{-1} and the region was 1180−950 cm^{-1}. Three major component peaks (peak 1, ca. 1184−1132 cm^{-1}; peak 2, ca. 1129−1066 cm^{-1}; and peak 3, ca. 1066−949 cm^{-1}) associated with the CHO regions were assessed for peak area and height intensity.

In the pericarp region, the peak area intensity of the cellulosic compounds (ca. 1290−1197 cm^{-1}) and total CHO (ca. 1192−876 cm^{-1}) were analyzed. Peak area intensity ratio was obtained by the height or area under one functional group/biological component band or area under

Table 2. Rumen Degradation Characteristics and Predicted Nutrient Availability of the Oats: Comparison of Newly Developed SO-I Oats with Normal Oats (Dancer and Derby) Grown at the University of Saskatchewan Research Station (Saskatoon) in 2006[a]

	oats			
item	Dancer	Derby	SO-I (super oats)	SEM
rumen degradation kinetics of dry matter (DM) (Qskov model)				
S (g/kg)	173 a	159 ab	109 b	1.3
D (g/kg)	597	574	600	2.4
U (g/kg)	230 a	267 ab	291 b	1.2
K_d (%/h)	46	44	45	3.6
RUDM (g/kg of DM)	300 a	337 b	362 b	7.7
EDDM (g/kg of DM)	700 a	663 b	638 b	7.7
rumen degradation kinetics of starch (ST) (DVE/OEB model)				
S (g/kg)	136 a	213 b	209 a	1.5
D (g/kg)	864 a	787 b	791 b	1.5
K_d (%/h)	55	51	50	3.0
BST (g/kg of DM)	46	41	47	1.9
EDST (g/kg of DM)	422 a	349 b	405 c	1.9
rumen degradation kinetics of protein (CP) (Qskov model)				
S (g/kg)	232	208	170	16.5
D (g/kg)	687	700	716	21.7
U (g/kg)	81	92	115	8.0
K_d (%/h)	42	39	49	2.5
BCP (g/kg of DM)	22 a	24 b	27 c	0.2
RUP (g/kg of DM)	20 a	22 b	25 c	0.2
EDCP (g/kg of DM)	100 a	95 b	103 c	0.2
modeling nutrient supply to dairy cattle				
(1) truly absorbed rumen undegraded feed protein in the small intestine (ARUP, g/kg of DM)				
ARUP (DVE/OEB system)	19 a	20 b	23 c	0.2
ARUP (NRC 2001 model)	17 a	18 b	21 c	0.2
(2) truly absorbed rumen synthesized microbial protein in the small intestine (AMCP, g/kg of DM)				
AMCP (DVE /OEB system)	64 a	60 b	58 b	0.6
AMCP (NRC 2001 model)	54 a	51 b	56 c	0.1
(3) total truly absorbed protein in the small intestine or total metabolizable protein supply (DVE or MP, g/kg of DM)				
DVE (= AMCP + ARUP − ENDP)	68	63	63	1.3
MP (= AMCP + ARUP + AECP)	76 a	74 b	81 c	0.1
(4) protein degraded balance (OEB or PDB g/kg DM)				
OEB (DVE/OEB system)	−2 a	−2 a	9 b	1.1
PDB (NRC 2001 model)	−12 a	−18 b	−13 a	0.2

[a] Means with the same letter in the same row are not significantly different ($P > 0.05$); SEM, standard error of mean.

Table 3. Structural Characteristics of Protein Amide I, Amide II, and Their Ratios in the Endosperm of Oats, Revealed Using SRFTIRM: Comparison of the Newly Developed SO-I with Two Normal Oat Varieties (Derby and Dancer) (IR Absorbance Unit)

	protein amide I and amide II[a]					
item:	protein amide I		protein amide II		protein amide I and II area	ratio of protein amide I to II
amide peak position: oat variety	∼1650 cm^{-1} (peak area)	∼1650 cm^{-1} (peak height)	∼1550 cm^{-1} (peak area)	∼1550 cm^{-1} (peak height)	∼1745−1485 cm^{-1}	∼1650−∼1550 cm^{-1}
Dancer	10.38	0.13 a	7.30	0.04	13.26	2.88
Derby	17.04	0.22 b	4.86	0.07	22.19	4.43
SO-I	14.02	0.21 ab	4.29	0.07	18.38	3.40
SEM[b]	2.140	0.023	2.940	0.011	2.845	0.716

[a] Protein amide data unit, IR absorbance unit; protein peak baseline, 1728−1483 cm^{-1}; protein amide I area region, 1745−1579 cm^{-1}; protein amide II area region, 1579−1485 cm^{-1}. [b] SEM, pooled standard error of means. Means with the same letter in the same column are not significantly different ($P > 0.05$).

another functional group band, which represented the biological component ratio intensity and distribution in the seed.

Multivariate Molecular Spectral Analysis. Agglomerative hierarchical cluster analysis (CLA) and principal component analysis (PCA) were performed using Statistica 7.0 software to clarify if these oat varieties differed in molecular chemical makeup. For CLA, Ward's algorithm method was used without any prior parametrization of the spectral data. For the PCA, the first three principal components (PC1, PC2, and PC3) were plotted. Detailed discussions on CLA and PCA applications in feed structure and feed molecular chemistry research have been reported (*14*, *15*, *23*, *24*).

Statistical Analysis. Statistical analyses were performed using the Mixed Model procedure of the SAS by generalized least-squares analysis (GLSA). Multitreatment comparisons were done using Fisher's protected LSD method. Significance was declared at $P < 0.05$.

RESULTS

Detecting Differences in Chemical Profiles, Protein Fraction, Biodegradation Kinetics, and Nutrient Supply: Comparison between New SO-I Oats and Conventional Oats. Chemical and protein

fraction profiles, rumen biodegradation kinetics, and predicted nutrient supply and availability for Dancer, Derby, and SO-I oats are presented in **Table 1**. SO-I contained higher (>10% unit) CFat, ADF, NDF, and SCP than Dancer and Derby oats. Contrary to this, SO-I oat contained lower (<10% unit) ADL than Dancer and Derby oats. In particular, ADL of SO-I (21 g/kg of DM) was lower by 47.5 and 36.4% units compared to the values of Dancer (40 g/kg of DM) and Derby oats (33 g/kg of DM), respectively. Compared to Derby oat, SO-I contained higher NPN. However, SO-I and Derby were similar in NDICP and ADICP. SO-I contained relatively higher TDN (820 g/kg of DM) and energy values ($NE_{L3\times}$ = 7.8 MJ/kg of DM; NE_m = 8.4 MJ/kg of DM; NE_g = 5.6 MJ/kg of DM). A comprehensive study on the effects of growth year and oat varieties was reported (*7*)

In the in situ kinetic study, the extent and rate of degradation are the most important parameters to be determined (**Table 2**). For the degradation kinetics of DM, there was no difference in K_d ($P > 0.05$), but significant differences in RUDM and EDDM ($P < 0.05$) with lower EDDM in SO-I (638 g/kg of DM) and Derby (663 g/kg of DM) and higher RUDM in SO-I (362 g/kg of DM) and Derby (337 g/kg of DM) in comparison with Dancer. For the degradation kinetics of starch, there was no difference in K_d ($P > 0.05$), but significant differences in EDST ($P < 0.05$) with lower values in SO-I (405 g/kg of DM) and Derby (349 g/kg of DM) in comparison with Dancer (422 g/kg of DM). For the degradation kinetics of protein, again there was no difference in K_d ($P > 0.05$), but significant differences in BCP, RUP, EDCP ($P < 0.05$) with higher values in SO-I. In the nutrient supply prediction study, the new SO-I oat provided highest ARUP (21−23 g/kg of DM) and MP (81 g/kg of DM) ($P < 0.05$) as compared to Dancer and Derby oats (**Table 2**).

Table 4. Structural Characteristics of Carbohydrate (CHO) in the Endosperm in Terms of the Component Peak Areas and Height and Their Ratios of Oat Seeds, Detected with SRFTIRM: Comparison of the Newly Developed SO-I with Two Normal Oat Varieties (Derby and Dancer) (IR Absorbance Unit)

		carbohydrate component (CHO)[a]		
item:	carbohydrate	first peak	second peak	third peak (starch)
CHO component peak position: oat variety	~1180−800 cm^{-1} peak area	~1150 cm^{-1}	~1080 cm^{-1}	~1025 cm^{-1}
		based on CHO component peak area		
Dancer	122.80	13.33	24.11	72.32
Derby	158.13	18.70	31.11	91.04
SO-I	121.58	13.65	24.53	73.41
SEM[b]	16.795	2.005	3.200	9.971
		based on CHO component peak height		
Dancer		0.24	0.17	0.64
Derby		0.31	0.21	0.78
SO-I		0.25	0.21	0.75
SEM[b]		0.029	0.028	0.107

[a] Carbohydrate data unit: IR absorbance unit and the CHO peak baseline and region, 1180−800, 1180, and 950 cm^{-1}, respectively. The oat CHO in the endosperm region has three major component peaks with the first, second, and third peaks at 1150, 1080, and 1025 cm^{-1}, respectively. The first, second, and third peak regions are 1184−1132, 1129−1066, and 1066−949 cm^{-1}, respectively. [b] SEM, pooled standard error of means; means with the same letter in the same column are not significantly different ($P > 0.05$).

Detecting Structural Makeup Difference in Endosperm Region: Comparison between New SO-I Oats and Conventional Oats. *Univariate Spectral Analysis*. Oat varieties did not differ ($P > 0.05$) in the relative IR absorbed intensity peak area and height of amide I, amide II, and their ratios (**Table 3**), total CHO and its component peaks (1, 2, and 3) and their ratios (**Table 4**), or ratio of total amide I and II to CHO (**Table 5**) in the endosperm tissue. The only exclusion was the amide I peak height, which was lower ($P < 0.05$) for Dancer (0.13 vs 0.22 and 0.21, Derby and SO-I, respectively) compared to Derby and SO-I.

Multivariate Spectral Analysis. CLA revealed that (**Figures 2** and **4**) the structural makeup of endosperm tissue between the oat varieties were not fully distinguishable in protein amide I, amide II (ca. 1728−1483 cm^{-1}, **Figure 2**), and CHO (1184−809 cm^{-1}; **Figure 4**) of the endosperm tissue. The results suggested that the three oat varieties were not significantly different in endosperm amides I and II and CHO molecular structural makeup. **Figure 3** presents a scatter plot of the first principal component versus the second principal component (**Figure 3a**) and the third principal component (**Figure 3b**) of PCA of amide I and amide II spectra obtained from Dancer, Derby, and SO-I endosperm tissues within cellular dimension. The first, second, and third principal components explained 92.1, 5.5, and 1.8% of the total variance, respectively. PCA also showed that protein amide I and II spectra from the endosperm between the varieties cannot be grouped in separate ellipses by varieties. This indicated that the endosperm structural makeup of these varieties is not fully distinguishable.

In a similar fashion, the endosperm CHO structural makeups of these varieties were not fully distinguishable (**Figure 5**). The first three principal components explain 76.8, 17.6, and 3.4% of the total variation in the CHO molecular structural spectrum. **Figures 3** and **5** further show that with regard to endosperm tissue,

Table 5. Structural Characteristics of Carbohydrate (CHO) in the Endosperm in Terms of the CHO Component Peak Area and Height Ratios of Oat Seeds, Detected with SRFTIRM: Comparison of the Newly Developed SO-I with Two Normal Oat Varieties (Derby and Dancer) (IR Absorbance Unit)

	carbohydrate (CHO)[a]			ratio of amide I and II to CHO
item:	ratio of CHO peak 1 to peak 2	ratio of CHO peak 1 to peak 3	ratio of CHO peak 2 to peak 3	amide I and II, ~1728−1483 cm^{-1}
CHO component peak position: oat variety	~1150 cm^{-1}/~1080 cm^{-1}	~1150 cm^{-1}/~1025 cm^{-1}	~1080 cm^{-1}/~1025 cm^{-1}	carbohydrate, ~1180−800 cm^{-1}
	based on CHO component peak area			peak area
Dancer	0.57	0.18	0.33	0.11
Derby	0.60	0.20	0.34	0.15
SO-I	0.55	0.19	0.34	0.16
SEM[b]	0.019	0.006	0.014	0.030

[a] Carbohydrate data unit: IR absorbance unit and the CHO peak baseline and region, 1184−809, 1184, and 949 cm^{-1}, respectively. The oat CHO in the endosperm region has three major component peaks with the first, second, and third peaks at ca. 1150, 1080, and 1025 cm^{-1}, respectively. [b] SEM, pooled standard error of means; means with the same letter in the same column are not significantly different ($P > 0.05$).

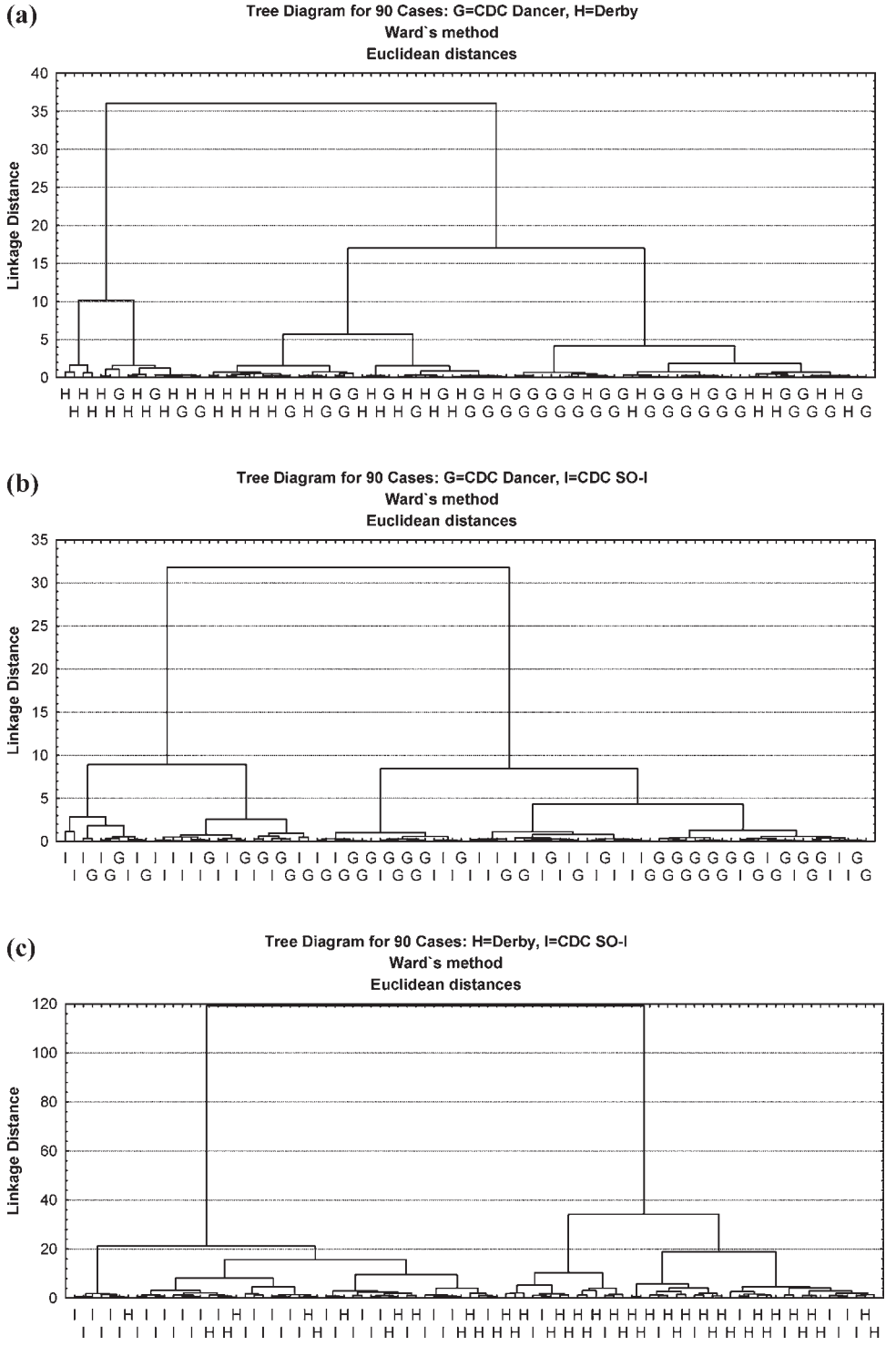

Figure 2. CLA cluster of synchrotron-based protein amide I and II spectra (ca. 1728−1483 cm^{-1}) obtained from oat grain endosperm regions at a cellular level (pixel size 10 μm × 10 μm): (**a**) Dancer (G) versus Derby (H); (**b**) Dancer (G) versus SO-I (I); (**c**) Derby (H) versus SO-I (I)] [CLA: (1) spectrum regions, ca. 1728−1483 cm^{-1}; (2) distance method, Euclidean; (3) cluster method, Ward's algorithm].

Dancer and SO-I overlapped greatly as compared to SO-I and Derby in protein and CHO molecular structural makeup.

Detecting Structural Makeup Difference in Pericarp Region: Comparison between New SO-I Oats and Conventional Oats. *Univariate Spectral Analysis*. **Table 6** shows the structural characteristics of cellulosic compound and total carbohydrate and their ratios in pericarp regions of Dancer, Derby, and SO-I oats. All three oat varieties were not different ($P > 0.05$) in cellulosic compound intensity (1.7, 1.6, and 1.9 for Dancer, Derby, and SO-I, respectively). SO-I was similar ($P > 0.05$) to Derby in total CHO peak area intensity (34.6 vs 30.9), peak height (0.24 vs 0.22), and ratio of cellulosic compound to CHO peak area (0.06 vs 0.05). The ratio of cellulosic compound to CHO peak height in the pericarp region ranged from 0.07 to 0.19 with the highest ($P < 0.05$) being in SO-I and intermediate in Derby (0.14).

Multivariate Spectral Analysis. **Figure 6** displays results of the CLA of spectra in the fingerprint region ca. 1775−800 cm^{-1} in the pericarp region of the oat grain in the form of a dendrogram. If the structural makeup differs among the plant varieties,

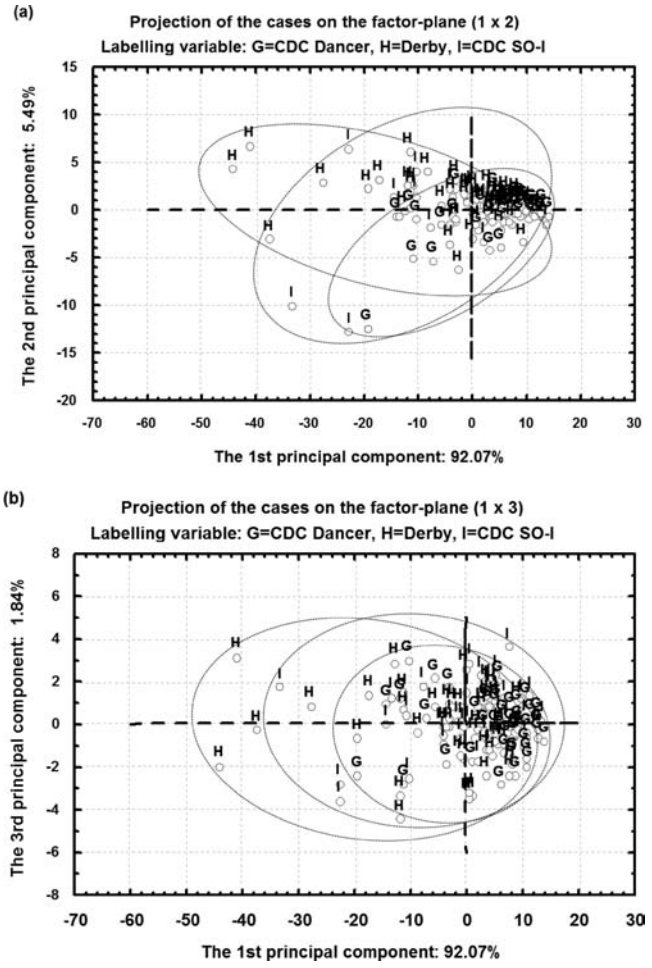

Figure 3. Scatter plot of the first principal component versus the second and third principal components of PCA of synchrotron-based protein amide I and II spectra (ca. 1728−1483 cm^{-1}) obtained from Dancer (G), Derby (H), and SO-I (I) oat endosperm regions at a cellular level (pixel size 10 μm × 10 μm) from all original spot spectra. The first, second, and third principal components explain 92.1, 5.5, and 1.8% of the total variance, respectively.

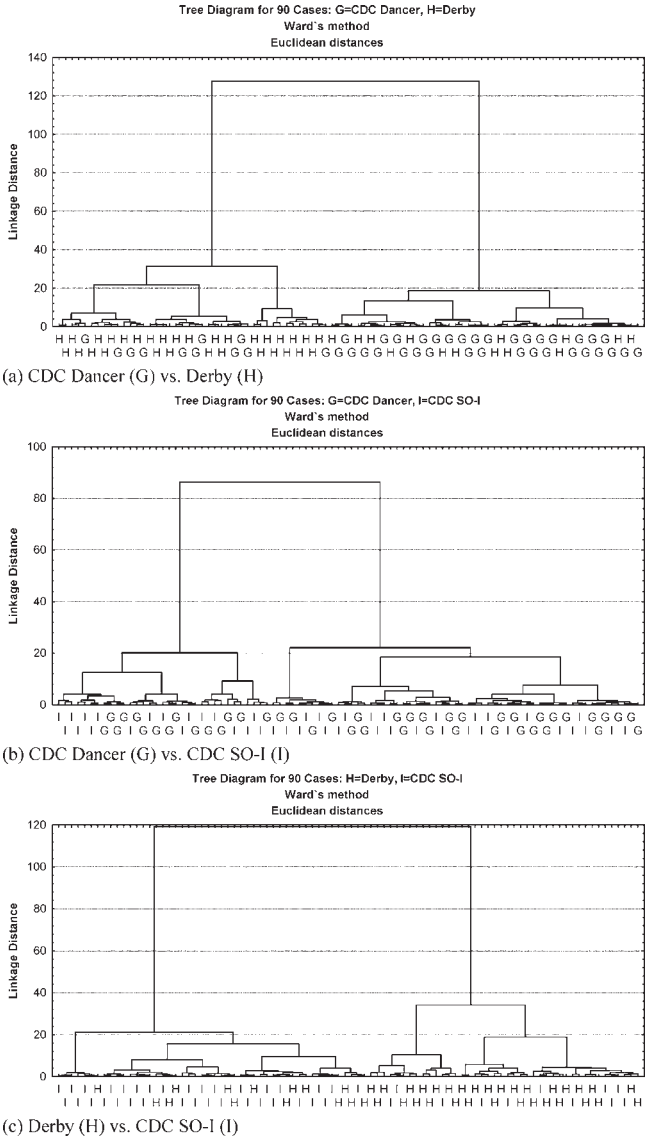

Figure 4. CLA cluster of synchrotron-based carbohydrate spectra (ca. 1184−809 cm^{-1}) obtained from oat grain endosperm regions at a cellular level (pixel size 10 μm × 10 μm): (**a**) Dancer (G) versus Derby (H); (**b**) Dancer (G) versus SO-I (I); (**c**) Derby (H) versus SO-I (I)] [CLA: (1) spectrum regions, ca. 1184−809 cm^{-1}; (2) distance method, Euclidean; (3) cluster method, Ward's algorithm].

the patterns of their spectra will be different. Initially, if the spectra differ among plants, they will form separate groups by oat varieties when spectral data sets are subjected to multivariate analysis. Our result shows spectral clusters between Dancer and Derby (**Figure 6a**) in pericarp regions were different, with a linkage distance of <5 and Derby and Dancer forming different separate groups. The Dancer group forms one distinct group just below a linkage distance of 2. The Derby group forms one distinct group below a linkage of 5, whereas these two groups form a single group at a linkage distance of about 27. Greater linkage distance between clusters of two varieties means the chance of similarity of these varieties is very low. Overall, Dancer and Derby oats were distinguished, which indicated their structural makeup were different. Panels **b** and **c** of **Figure 6** show that SO-I versus Dancer or SO-I versus Derby did not form different clusters, indicating similarity in structural makeup.

PCA (**Figure 7**) indicated that the pericarp structural chemical makeup of Dancer and Derby are fully distinguishable. PC1, PC2, and PC3 individually explain 78.3, 7.9, and 4.0% of the total variance, respectively. SO-I and Dancer can be almost grouped in separate ellipses, but SO-I and Derby could not be grouped into separate ellipses.

DISCUSSION

Chemical Profiles, Protein Fraction, Biodegradation Kinetics, and Nutrient Supply: Comparison between New SO-I Oats and Conventional Oats. Oat grain refers to the entire kernel, hull and groat inclusive. Major tissues of groat are endosperm, embryo, and germ. The percentages of groat in Dancer, Derby, and SO-I are 80.4, 61.3, and 62.0%, respectively, resulting in hull contents of 19.6, 38.7, and 38.0% (*6*). As the present study indicates, Dancer had lower ADF and greater starch contents than Derby and SO-I oats. The major differences of SO-I oat in terms of chemical content from conventional oat varieties are its lower lignin (ADL) and higher fat contents. A significant difference in effective degradability (EDDM, EDST) was detected between the oat varieties. These results indicate that measuring DM degradation kinetics may not be indicative of the extent of starch digestion, analogous to the findings of Ramsey et al. (*25*) on barley. No variation in fermentation rate occurred among the varieties of oat. Because lipids yield more than twice as much

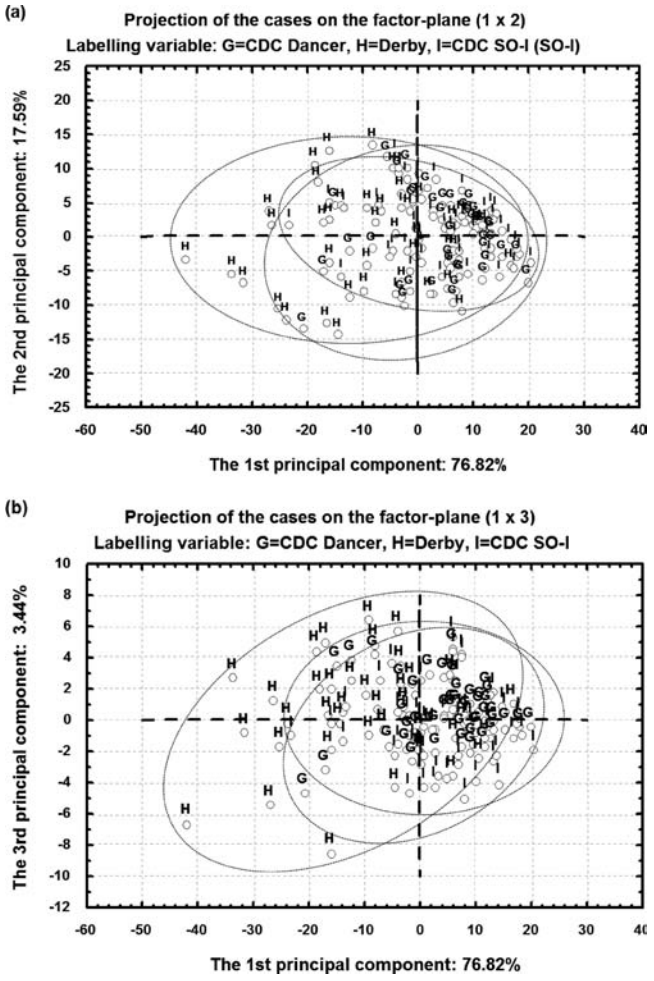

Figure 5. Scatter plot of the first principal component versus the second and third principal components of PCA of synchrotron-based carbohydrate spectra (ca. 1184−809 cm^{-1}) obtained from Dancer (G), Derby (H), and SO-I (I) oat endosperm regions at a cellular level (pixel size 10 μm × 10 μm) from all original spot spectrum. For CHO, the first, second, and third principal components explain 76.8, 17.6, and 3.4% of the total variance, respectively.

available energy per unit compared to carbohydrates or protein, the higher lipid content of SO-I grain is an advantage over Dancer and Derby oats in terms of energy content. Peterson and Wood (*26*) stated that higher oil content is negatively correlated with starch content, caused by a portion of the reduced carbon redirected from starch into oil synthesis in high-oil oat varieties. However, in the present study, differences in lipid levels among the three varieties were not reflected much in starch: SO-I (452 g/kg of DM) was not significantly lower than Dancer (468 g/kg of DM) and was even higher than Derby oat (389 g/kg of DM) in starch content. Welch (*27*) cited several studies from Europe and North America that observed significant negative correlations between protein and lipid contents of oat grains. However, in the present study, we did not find a consistent inverse relationship between oat protein and lipid contents. The National Research Council gave a TDN of 785 g/kg of DM for oat grain; using the same National Research Council calculations, Dancer (797), Derby (801), and SO-I (820 g/kg of DM) had greater TDN. According to the DVE/OEB and NRC systems, SO-I had a slightly lower organic matter fraction, which is fermentable in the rumen, and greater metabolizable protein (MP). Both Dancer and Derby oats had negative OEB values, indicating a potential shortage of N in the rumen. In contrast, SO-I oat had a positive OEB value. Although there was an interaction of the nutrient contents and varieties, overall, Derby and SO-I were relatively similar in rumen degradation characteristics and predicted nutrient availability aspects.

Detecting Structural Makeup Difference: Comparison between New SO-I Oats and Conventional Oats. Recent studies have explored the application of SRFTIRM to the study of feed samples. Molecular imaging of corn and barley (*28*) has been carried out to reveal spatial intensity and distribution of chemical functional groups within the intact tissue. Such information is useful for relating nutrient utilization and digestion characteristics with the specific chemical makeup of the cereal grain (*29*). The protein structure profile (α-helix, β-sheet, randon coil) has been studied in feather protein (*30*). Yu et al. (*13*) also used SRFTIRM to compare the nonstructural carbohydrate−starch and protein matrix of Harrington and Valier barley with reference to differences in their physical digestibility characteristics. However, no publication was found regarding inherent structural

Table 6. Structural Characteristics of Carbohydrate (CHO) in the Pericarp in Terms of the Component Peak Areas and Height and Their Ratios of Oat Seeds, Detected with SRFTIRM: Comparison of the Newly Developed SO-I with Two Normal Oat Varieties (Derby and Dancer) (IR Absorbance Unit)

	carbohydrate component (CHO)[a]		
items:	cellulosic compounds	total carbohydrate	ratio of cellulosic compound to total carbohydrate
CHO component peak region: oat variety	~1290−1197 cm^{-1}	~1192−876 cm^{-1}	~1290−1197 cm^{-1}/~1192−876 cm^{-1}
		based on peak area	
Dancer	1.70	89.22 a	0.02 a
Derby	1.56	30.91 b	0.05 b
SO-I	1.89	34.57 b	0.06 b
SEM[b]	0.151	3.842	0.005
		based on peak height	
Dancer	0.04 a	0.60 a	0.07 a
Derby	0.03 b	0.22 b	0.14 b
SO-I	0.04 a	0.24 b	0.19 c
SEM[b]	0.003	0.024	0.008

[a] Carbohydrate data unit: IR absorbance unit. [b] SEM, pooled standard error of means; means with the same letter in the same column are not significantly different ($P > 0.05$).

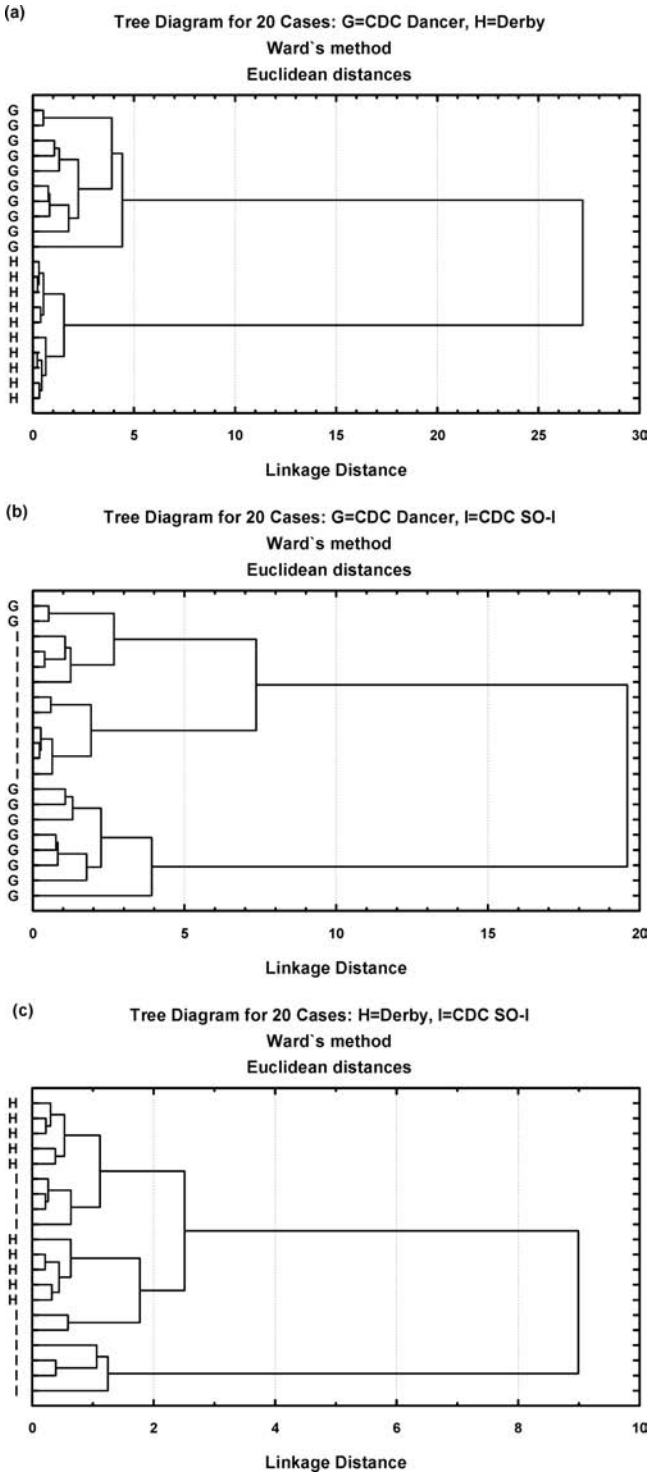

Figure 6. CLA cluster of synchrotron-based fingerprint spectra (ca. 1775−800 cm^{-1}) obtained from the pericarp regions of the three oat varieties, (**a**) Dancer versus Derby, (**b**) Dancer versus SO-I, and (**c**) Derby versus SO-I, at a cellular level (pixel size 10 × 10 μm) [CLA: (1) spectrum regions, ca. 1775−800 cm^{-1}; (2) distance method, Euclidean; (3) cluster method, Ward's algorithm].

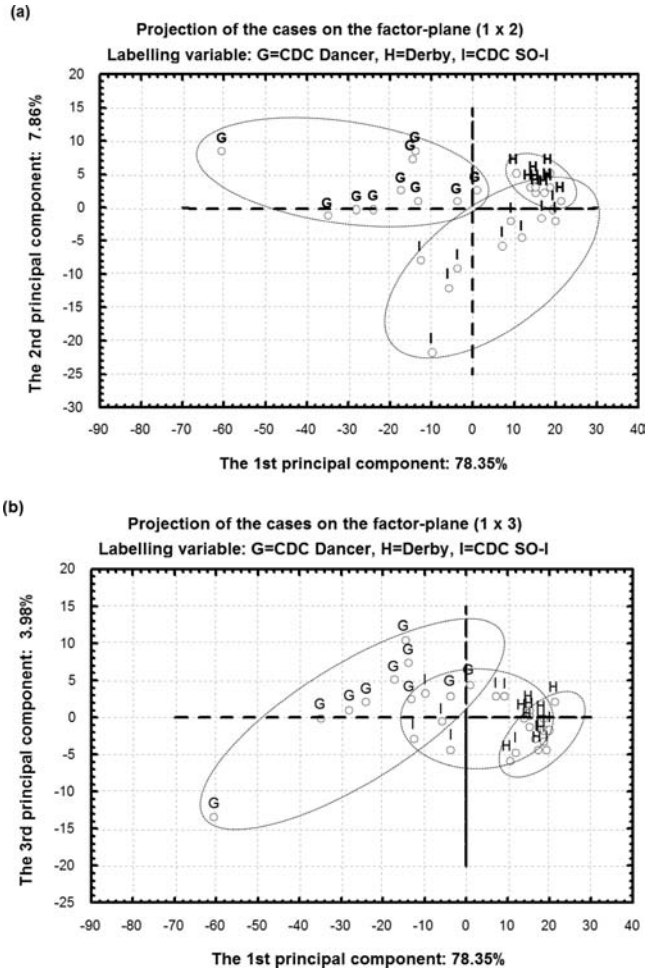

Figure 7. Scatter plot of the first principal component versus the second and third principal components of PCA of synchrotron-based fingerprint region spectra (ca.1775−800 cm^{-1}) obtained from Dancer (G), Derby (H), and SO-I (I) oat pericarp regions at a cellular level (pixel size 10 μm × 10 μm) from all original spot spectra. The first, second, and third principal components explain 78.4, 7.9, and 4.0% of the total variance, respectively.

makeup of oat grains and their correlation with the nutritive value from different varieties of oat. Both uni- and multivariate spectral analyses revealed that Dancer, Derby, and SO-I were not significantly different in terms of amides I and II and CHO peak intensity within cellular dimensions in the endosperm tissues. Protein within the endosperm tissue of cereal grains is arranged in a matrix that surrounds and protects the starch granules, making them less available for digestion by rumen bacteria (*31*). This may be a major factor responsible for differences in rumen starch degradation among different grain varieties. If more protein within the grain endosperm relates to a stronger protein matrix, higher protein content should indicate a larger degree of "protection", which would be related to a reduction in the rate and extent to which starch is able to be degraded. Therefore, a lower starch to protein ratio may be indicative of a greater degree of protection of starch granules within the protein matrix, resulting in a lower rate and extent of rumen degradation (*21*). As previously reported, the starch to protein IR absorbed intensity ratio was larger for Dancer than for Derby and SO-I oats, suggesting that for Dancer the endosperm tissue structural chemical makeup is slightly more heterogeneous and less densely packed in the protein matrix, relative to Derby and SO-I. The heterogeneities of SO-I and Derby oats in their endosperm tissue chemical makeup are more similar; furthermore, this implies that the starch granules could be more closely associated with the protein matrix in these two oat varieties than in Dancer. Although SO-I contained higher starch, similar to Dancer, the starch to protein ratio was lower, which was similar to Derby. Thus, the results suggested that investigation of feed components' structural makeup in plant fragment in cellular and subcellular levels, through SRFTIRM, can provide more useful information to clarify the contribution of different

parts of a particular grain on the nutritive value of feed. With this knowledge, grains that have more desirable feeding qualities may be selected and used in the formulation of feed rations. Overall, as the present study indicated, the chemical structural makeup of SO-I is very similar to that of Derby for the pericarp region and to that of Dancer for the endosperm tissue. Such a unique inherent feature of SO-I in terms of structural makeup within the grain kernel is probably involved with its superior nutritive value compared with other available oat varieties.

In conclusion, comparison between the new genotype oats and conventional oats showed (1) differences in basic chemical and protein subfraction profile and energy values, with the new SO-I oat containing lower lignin and higher soluble crude protein, crude fat, and energy values; (2) significant differences in rumen biodegradation kinetics; (3) significant differences in nutrient supply with highest truly absorbed rumen undegraded protein (ARUP) and total metabolizable protein supply (MP) from the new SO-I oats; and (4) significant differences in structural makeup in terms of protein amide I in the endosperm region and cellulosic compounds to carbohydrate ratio in the pericarp region. The results suggest that with the SRFTIRM technique, the structural makeup differences between the new genotype oats (SO-I) and two conventional oats (Dancer and Derby) could be revealed. SRFTIRM has great potential to assess intrinsic molecular structure and biopolymer conformation.

ABBREVIATIONS USED

ABCP, truly absorbed bypass protein in the small intestine; ADF, acid detergent fiber; ADICP, acid detergent insoluble crude protein; ADL, acid detergent lignin; AMCP, truly absorbed microbial protein in the small intestine; ARUP, truly absorbed rumen undegraded protein in the small intestine; BCP, rumen bypass feed protein estimated from the DVE/OEB system; CFat, crude fat; CHO, total carbohydrate; D, insoluble, but potentially degradable, fraction in the in situ incubations; DM, dry matter; DVE, truly digested protein in the small intestine; ED, effective degradation of feed DM, CP or starch (EDDM, EDCP and EDST); K_d, rate of degradation of D fraction (%/h); ME, metabolizable energy estimated from NRC model 2001; $ME_{3\times}$, metabolizable energy at production level of intake estimated (NRC model 2001); MP, total metabolizable protein (NRC, 2001); NDF, neutral detergent fiber; NDICP, neutral detergent insoluble crude protein; $NE_{L3\times}$, net energy for lactation at production level of intake estimated (NRC model 2001); NE_m, net energy for maintenance estimated from NRC model 1996; NE_g, net energy for growth estimated from NRC model 1996; NPN, nonprotein nitrogen; NSC, nonstructural carbohydrates; OEB, degraded protein balance (DVE/OEB system); PA, fraction of CP that is instantaneously solubilized at time zero; PB1, fraction of CP that is fast degradable in the rumen; PB2, fraction of CP that is intermediately degradable in the rumen; PB3, fraction of CP that is slowly degradable in the rumen; PC, fraction of CP that is undegraded; PDB, degraded protein balance (NRC 2001 model); RUP, rumen undegraded feed protein; RUST, rumen undegraded feed starch; S, soluble fraction in the in situ incubation; SCP, soluble crude protein; $TDN_{1\times}$, total digestible nutrient; T_0, lag time in which no degradation takes place (h); U, undegradable fraction in the in situ incubation.

ACKNOWLEDGMENT

We are grateful to B. Rossnagel (University of Saskatchewan) for providing seed samples, Z. Niu (University of Saskatchewan) for chemical analysis and in situ work, and Jennifer Bohon, Nebojsa Marinkovic, and Lisa Miller (NSLS-BNL, U.S. Department of Energy, New York) for helpful data collection at U2B and U10B experimental stations.

LITERATURE CITED

(1) *Statistics Canada. The Daily. Principal Field Crops*, available at http://www.statcan.gc.ca/daily-quotidien/080507/dq080507a-eng.htm, accessed February 12, **2009**.

(2) Truswell, A. S. Cereal grains and coronary heart disease. Review. *Eur. J. Clin. Nutr.* **2002**, *56*, 1–14.

(3) Moran, J. B. Cereal grains in complete diets for dairy cows: a comparison of rolled barley, wheat and oats and of three methods of processing oats. *Anim. Prod.* **1986**, *43*, 27–36.

(4) Crosbie, G. B.; Tarr, A. W.; Portmann, P. A.; Rowe, J. B. Variation in hull composition and digestibility among oat genotypes. *Crop Sci.* **1985**, *25*, 678–680.

(5) Ekern, A.; Havrevoll, O.; Haug, A.; Berg, J.; Lindstad, P.; Skeie, S. Oat and barley based concentrate supplements for dairy cows. *Acta Agric. Scand., Sect. A, Anim. Sci.* **2003**, *53*, 65–73.

(6) Fuhr, L. G. M. *Low lignin hull, high oil groat oat grain*. M.S. thesis, University of Saskatchewan, Saskatoon, SK, Canada, **2006**.

(7) Yu, P.; Rossnagel, B. G.; Niu, Z. Protein value of a new genotype oat (CDC SO-I) for the NRC dairy model: protein degradation balance and kinetics, protein fractions and total metabolizable protein supply. *Can. J. Anim. Sci.* **2008**, *88*, 507–513.

(8) Yu, P. Application of advanced synchrotron radiation-based Fourier transform infrared (SR-FTIR) microspectroscopy to animal nutrition and feed science: a novel approach. *Br. J. Nutr.* **2004**, *92*, 869–885.

(9) Orskov, E. R.; McDonald, I. The estimation of protein degradability in the rumen from incubation measurements weighted according to the rate of passage. *J. Agric. Sci.* **1979**, *92*, 499–503.

(10) AOAC. *Official Methods of Analysis*, 15th ed.; Association of Official Analytical Chemists: Arlington,VA, 1990.

(11) Van Soest, P. J.; Robertson, J. B.; Lewis, B. A. Carbohydrate methodology, metabolism and nutritional implications in dairy cattle. Methods for dietary fiber, neutral detergent fiber and nonstarch polysaccharides in relation to animal nutrition. *J. Dairy Sci.* **1991**, *74*, 3583–3597.

(12) Tamminga, S.; Van Straalen, W. M.; Subnel, A. P. J.; Meijer, R. G. M.; Steg, A.; Wever, C. J. G.; Block, M. C. The Dutch protein evaluation system: the DVE/OEB-system. *Livest. Prod. Sci.* **1994**, *40*, 139–155.

(13) Yu, P.; Christensen, D. A.; Christensen, C. R.; Drew, M. D.; Rossnagel, B. G.; McKinnon, J. J. Use of synchrotron FTIR microspectroscopy to identify chemical differences in barley endosperm tissue in relation to rumen degradation characteristics. *Can. J. Anim. Sci.* **2004**, *84*, 524–527.

(14) Sockalingum, G. D.; Bouhedja, W.; Pina, P.; Allouch, P.; Bloy, C.; Manfait, M. FT-IT spectroscopy as an emerging method for rapid characterization of microorganisms. *Cell. Mol. Biol.* **1998**, *44*, 261–269.

(15) Yu, P. Synchrotron-based microspectroscopic analysis of molecular and biopolymer structures using multivariate techniques and advanced multi-components modeling. *Can. J. Anal. Sci. Spectrosc.* **2008**, *53*, 220–231.

(16) Himmelsbach, D.; Khalili, S.; Akin, S.; FT-IR, D. E. Microspectroscopic imaging of flax (*Linum usitatissimum* L.) stems. *Cell. Mol. Biol.* **1998**, *44*, 99–108.

(17) Wetzel, D. L.; Eilert, A. J.; Pietrzak, L. N.; Miller, S. S.; Sweat, J. A. Ultraspatially resolved synchrotron infrared microspectroscopy of plant tissue in situ. *Cell. Mol. Biol.* **1998**, *44*, 145–167.

(18) Wetzel, D. L.; Srivarin, P.; Finney, J. R. Revealing protein infrared spectral detail in a heterogeneous matrix dominated by starch. *Vibr. Spectrosc.* **2003**, *31*, 109–114.

(19) Jackson, M.; Mantsch, H. H. Infrared spectroscopy ex vivo tissue analysis. In *Biomedical Spectroscopy*, **2000**.

(20) Marinkovic, N. S.; Huang, R.; Bromberg, P.; Sullivan, M.; Toomey, J.; Miller, L. M.; Sperber, E.; Moshe, S.; Jones, K. W.; Chouparova, E.; Lappi, S.; Franzen, S.; Chance, M. R. Center for Synchrotron

Biosciences' U2B beamline: an international resource for biological infrared spectroscopy. *J. Synchrotron Radiat*. **2002**, *9*, 189–197.
(21) Marinkovic, N. S.; Chance, M. R. Synchrotron infrared microspectroscopy. In *Encyclopedia of Molecular Cell Biology and Molecular Medicine*, 2nd ed.; Meyers, R., Ed.; Wiley: New York, 2005; Vol. 13, pp 671−708.
(22) Miller, L. M.; Dumas, P. Chemical imaging of biological tissue with synchrotron infrared light. *Biochim. Biophys. Acta* **2006**, *1758*, 846–857.
(23) Yu, P.; Doiron, K.; Liu, D. Shining light on the differences in molecular structural chemical makeup and the causes of distinct degradation behavior between malting- and feed-type barley using synchrotron FTIR microspectroscopy: a novel approach. *J. Agric. Food Chem*. **2008**, *56*, 3417–3426.
(24) Yu, P.; Block, H. C.; Doiron, K. Understanding the differences in molecular conformation of carbohydrate and protein in endosperm tissues of grains with different biodegradation kinetics using advanced synchrotron technology. *Spectrochim. Acta Part A: Biomol. Spectrosc*. **2009**, *7*, 1837–1844.
(25) Ramsey, P. B.; Mathison, G. W.; Goonewardene, L. A. Relationships between ruminal dry matter and starch disappearance and apparent digestibility of barley grain. *Anim. Feed Sci. Technol*. **2001**, *94*, 155–170.
(26) Peterson, D. M.; Wood, D. F. Composition and structure of high-oil oat. *J. Cereal Sci*. **1997**, *26*, 121–128.
(27) Welch, R. W. The chemical composition of oats. *The Oat Crop: Production and Utilization*; Welch, R. W., Ed.; Chapman and Hall: New York, 1995; pp 279−320
(28) Yu, P.; McKinnon, J. J.; Christensen, C. R.; Christensen, D. A. Using synchrotron transmission FTIR microspectroscopy as a rapid, direct and non-destructive analytical technique to reveal molecular microstructural-chemical features within tissue in grain barley. *J. Agric. Food Chem*. **2004**, *52*, 1484–1494.
(29) Doiron, J. J.; Yu, P.; McKinnon, J. J.; Christensen, D. A. Heat-induced protein structures and protein subfractions in relation to protein degradation kinetics and intestinal availability in dairy cattle. *J. Dairy Sci*. **2009**, *92*, 3319–3330.
(30) Yu, P.; McKinnon, J. J.; Christensen, C. R.; Christensen, D. A. Using synchrotron FTIR microscopy to reveal chemical features of feather protein secondary structure, comparison with other feed protein sources. *J. Agric. Food Chem*. **2004**, *52*, 7353–7361.
(31) McAllister, T. A.; Phillippe, R. C.; Rode, L. M.; Cheng, K. J. Effect of the protein matrix on the digestion of cereal grains by ruminal microorganisms. *J. Anim. Sci*. **1993**, *71*, 205–212.

Received for review October 12, 2009. Revised manuscript received January 7, 2010. Accepted January 08, 2010. This research has been supported by grants from the Natural Sciences and Engineering Research Council of Canada (NSERC, Individual Discovery Grant), the Saskatchewan Agricultural Development Fund (ADF), and the Ministry of Saskatchewan Agriculture Chair Fund (SRP Program Chair). The National Synchrotron Light Source at Brookhaven National Laboratory (NSLS-BNL, U.S. Department of Energy, New York) is supported by the U.S. Department of Energy, Contract DE-AC02-98CH10886.